

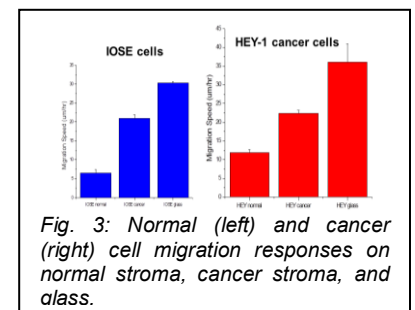
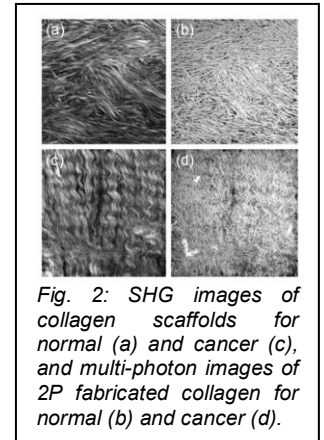
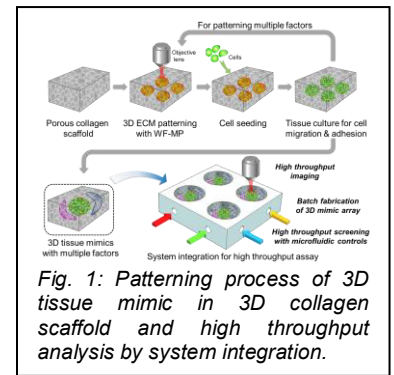
CP8*: Extracellular matrix regulation for precision medicine: Paul Campagnola, Manish Patankar, U. of Wisconsin; **Funding Source and Period:** NHLBI 5R21HL126190-02 2015-2017 (Campagnola, PI),

Associated With: TRD1,2,3,4

Significance: Campagnola laboratory is a leader in developing bioimaging techniques to study the role of extracellular matrix (ECM) in pathogenesis; his lab further pioneered microfabrication techniques for creating biomimetic cell culture platforms that recapitulate the native 3D tissue ECM environment (1-24). The ECM directs cell shape, spreading, differentiation, migration, and proliferation in addition to providing structural support (25-29) by presenting a complex milieu of topographic, mechanical and biochemical cues to cells. For example, adhesion and migration are known to become mis-regulated during ovarian and other cancers (30, 31). It is recognized that the response of a patient to a particular treatment or a particular drug will be very different from that of another person due to the unique genotype and phenotype. In drug selection for disease treatment, tissue mimics created from a patient's own cells growing on ECM mimics that recreate the patient's tissue morphology may allow clinicians to select the most effective drug on a rational basis instead of today's trial-and-error approach. As an example, for ovarian cancer treatment, one may envision cancer and stromal cells extracted during biopsy may be expanded, and patterned into tissue mimics in a fully humanized environment. These tissue mimics may be automatically cultured in microfluidic devices until they become morphologically "mature" lesions. A drugs panel at different dosages can be used to challenge these tissue mimics and to identify a precise dosing scheme (Fig. 1).

Approach: The native ECM has intrinsic 3D complexity with size features over length scales of a ~100 nm in diameter to several μm in length. The fabrication of these tissue mimics, to the fullest extent possible, needs to faithfully reproduce the nano/microstructured topography from the same multiple ECM components that comprise the in vivo structure. Recent work in the Campagnola lab in the U. of Wisconsin using multiphoton (MP) microfabrication has shown that a very effective way to create a biomimetic environment is to follow a "blueprint" based on high resolution microscopy imaging data (32) (Fig. 2). They have further demonstrated that cells grown in these biomimetic environments exhibit more realistic proliferation rates and migration dynamics (speed and directionality; (Fig. 3)) as compared with less native environments. Working with ovarian cancer expert, Dr. Patankar (33-40), they further showed the normal and ovarian cancer cell phenotype can be modified just by varying their scaffold morphology. LBRC will adapt Campagnola's microfabrication approach and will attempt to increase fabrication speed by at least two orders of magnitude using wide field temporal focusing approach extending a well proven technique in our laboratory (41). The increased fabrication speed will be obtained from parallelization of excitation beam. The benchmark for transferring the point scanning technology to wide-field system will be 90% fidelity verified by 3D imaging. Working with Campagnola, we will use these scaffolds to establish a drug assay protocol and demonstrate differential response of ovarian cancer cells to cisplatin, oxaliplatin, arsenite, or taxol and combinations thereof under different stromal compositions and morphologies.

Push-Pull Relationship: For developing tissue mimics to enable precision medicine, LBRC **pushes** high throughput microfabrication techniques to increase fabrication efficiency (TRD1.2). The Wisconsin labs hypothesize that ECM features below current fabrication resolution can also influence cellular phenotype **pulling** LBRC to develop structured light interferometric fabrication processes targeting 200 nm level isotropic resolution. For cellular phenotype characterization on these tissue mimics, LBRC further **pushes** enhanced resolution multimodal Raman and phase microscopy to quantify cellular biomechanics and biochemistry (TRD2.1, 3.1) in vivo. In ex vivo, this system will allow us to quantify mRNA expression profile by labeling with a small panel of SERS nanoprobe (TRD4). These probes with distinct Raman signatures will be conjugated with RNA oligos that are complementary to genes of interest (TRD3.1). The need for quantifying an increasing larger panel of genes will **pull** LBRC toward developing even high throughput single cell mRNA profiling based on developing a larger panel of SERS nanoparticles (TRD4) and higher throughput and higher resolution Raman confocal imaging (TRD3.1) as an alternative to the more labor-intensive fluorescence approach(42).



Literature Cited:

1. Williams JC, Campagnola PJ. Wearable Second Harmonic Generation Imaging: The Sarcomeric Bridge to the Clinic. *Neuron*. 2015;88(6):1067-9. doi: 10.1016/j.neuron.2015.12.009. PubMed PMID: 26687213.
2. Wen B, Campbell KR, Cox BL, Eliceiri KW, Superfine R, Campagnola PJ. Multi-view second-harmonic generation imaging of mouse tail tendon via reflective micro-prisms. *Opt Lett*. 2015;40(13):3201-4. doi: 10.1364/OL.40.003201. PubMed PMID: 26125402; PubMed Central PMCID: PMC4979975.
3. Da Sie Y, Li YC, Chang NS, Campagnola PJ, Chen SJ. Fabrication of three-dimensional multi-protein microstructures for cell migration and adhesion enhancement. *Biomed Opt Express*. 2015;6(2):480-90. doi: 10.1364/BOE.6.000480. PubMed PMID: 25780738; PubMed Central PMCID: PMC4354577.
4. Chaudhary R, Campbell KR, Tilbury KB, Vanderby R, Jr., Block WF, Kijowski R, Campagnola PJ. Articular cartilage zonal differentiation via 3D Second-Harmonic Generation imaging microscopy. *Connect Tissue Res*. 2015;56(2):76-86. doi: 10.3109/03008207.2015.1013192. PubMed PMID: 25738523; PubMed Central PMCID: PMC4497507.
5. Wen BL, Brewer MA, Nadiarnykh O, Hocker J, Singh V, Mackie TR, Campagnola PJ. Texture analysis applied to second harmonic generation image data for ovarian cancer classification. *J Biomed Opt*. 2014;19(9):096007. doi: 10.1117/1.JBO.19.9.096007. PubMed PMID: 26296156; PubMed Central PMCID: PMC4161736.
6. Tilbury K, Lien CH, Chen SJ, Campagnola PJ. Differentiation of Col I and Col III isoforms in stromal models of ovarian cancer by analysis of second harmonic generation polarization and emission directionality. *Biophys J*. 2014;106(2):354-65. doi: 10.1016/j.bpj.2013.10.044. PubMed PMID: 24461010; PubMed Central PMCID: PMC3907237.
7. Hall G, Tilbury KB, Campbell KR, Eliceiri KW, Campagnola PJ. Experimental and simulation study of the wavelength dependent second harmonic generation of collagen in scattering tissues. *Opt Lett*. 2014;39(7):1897-900. doi: 10.1364/OL.39.001897. PubMed PMID: 24686633; PubMed Central PMCID: PMC4487653.
8. Lien CH, Tilbury K, Chen SJ, Campagnola PJ. Precise, motion-free polarization control in Second Harmonic Generation microscopy using a liquid crystal modulator in the infinity space. *Biomed Opt Express*. 2013;4(10):1991-2002. doi: 10.1364/BOE.4.001991. PubMed PMID: 24156059; PubMed Central PMCID: PMC3799661.
9. Hanson KP, Jung JP, Tran QA, Hsu SP, Iida R, Ajeti V, Campagnola PJ, Eliceiri KW, Squirrell JM, Lyons GE, Ogle BM. Spatial and temporal analysis of extracellular matrix proteins in the developing murine heart: a blueprint for regeneration. *Tissue Eng Part A*. 2013;19(9-10):1132-43. doi: 10.1089/ten.TEA.2012.0316. PubMed PMID: 23273220; PubMed Central PMCID: PMC3609645.
10. Ajeti V, Lien CH, Chen SJ, Su PJ, Squirrell JM, Molinarolo KH, Lyons GE, Eliceiri KW, Ogle BM, Campagnola PJ. Image-inspired 3D multiphoton excited fabrication of extracellular matrix structures by modulated raster scanning. *OPT EXPRESS*. 2013;21(21):25346-55. doi: 10.1364/OE.21.025346. PubMed PMID: 24150376.
11. Su PJ, Tran QA, Fong JJ, Eliceiri KW, Ogle BM, Campagnola PJ. Mesenchymal stem cell interactions with 3D ECM modules fabricated via multiphoton excited photochemistry. *Biomacromolecules*. 2012;13(9):2917-25. doi: 10.1021/bm300949k. PubMed PMID: 22876971.
12. Lin CY, Lien CH, Cho KC, Chang CY, Chang NS, Campagnola PJ, Dong CY, Chen SJ. Investigation of two-photon excited fluorescence increment via crosslinked bovine serum albumin. *OPT EXPRESS*. 2012;20(13):13669-76. doi: 10.1364/OE.20.013669. PubMed PMID: 22714432.
13. Li YC, Cheng LC, Chang CY, Lien CH, Campagnola PJ, Chen SJ. Fast multiphoton microfabrication of freeform polymer microstructures by spatiotemporal focusing and patterned excitation. *OPT EXPRESS*. 2012;20(17):19030-8. doi: 10.1364/OE.20.019030. PubMed PMID: 23038543.

14. Hall G, Jacques SL, Eliceiri KW, Campagnola PJ. Goniometric measurements of thick tissue using Monte Carlo simulations to obtain the single scattering anisotropy coefficient. *Biomed Opt Express*. 2012;3(11):2707-19. doi: 10.1364/BOE.3.002707. PubMed PMID: 23162710; PubMed Central PMCID: PMC3493220.
15. Chen X, Raggio C, Campagnola PJ. Second-harmonic generation circular dichroism studies of osteogenesis imperfecta. *Opt Lett*. 2012;37(18):3837-9. PubMed PMID: 23041876; PubMed Central PMCID: PMC34337953.
16. Lien CH, Kuo WS, Cho KC, Lin CY, Su YD, Huang LL, Campagnola PJ, Dong CY, Chen SJ. Fabrication of gold nanorods-doped, bovine serum albumin microstructures via multiphoton excited photochemistry. *OPT EXPRESS*. 2011;19(7):6260-8. doi: 10.1364/OE.19.006260. PubMed PMID: 21451651.
17. Hall G, Spalding GC, Campagnola PJ, White JG, Eliceiri KW. Fast localized wavefront correction using area-mapped phase-shift interferometry. *Opt Lett*. 2011;36(15):2892-4. doi: 10.1364/OL.36.002892. PubMed PMID: 21808349; PubMed Central PMCID: PMC34487656.
18. Cho KC, Lien CH, Lin CY, Chang CY, Huang LL, Campagnola PJ, Dong CY, Chen SJ. Enhanced two-photon excited fluorescence in three-dimensionally crosslinked bovine serum albumin microstructures. *OPT EXPRESS*. 2011;19(12):11732-9. doi: 10.1364/OE.19.011732. PubMed PMID: 21716404.
19. Nadiarnykh O, LaComb RB, Brewer MA, Campagnola PJ. Alterations of the extracellular matrix in ovarian cancer studied by Second Harmonic Generation imaging microscopy. *BMC Cancer*. 2010;10:14. doi:10.1186/1471-2407-10-94. PubMed PMID: ISI:000275797700003.
20. Kuo WS, Lien CH, Cho KC, Chang CY, Lin CY, Huang LL, Campagnola PJ, Dong CY, Chen SJ. Multiphoton fabrication of freeform polymer microstructures with gold nanorods. *OPT EXPRESS*. 2010;18(26):27550-9. doi: 10.1364/OE.18.027550. PubMed PMID: 21197029.
21. Plotnikov S, Juneja V, Isaacson AB, Mohler WA, Campagnola PJ. Optical clearing for improved contrast in second harmonic generation imaging of skeletal muscle. *Biophys J*. 2006;90(1):328-39. PubMed PMID: 16214853.
22. Campagnola PJ, Loew LM. Second-harmonic imaging microscopy for visualizing biomolecular arrays in cells, tissues and organisms. *Nat Biotechnol*. 2003;21(11):1356-60. PubMed PMID: 14595363.
23. Campagnola PJ, Clark HA, Mohler WA, Lewis A, Loew LM. Second-harmonic imaging microscopy of living cells. *J Biomed Opt*. 2001;6(3):277-86. PubMed PMID: 11516317.
24. Campagnola PJ, Wei M-D, Lewis A, Loew LM. High-resolution nonlinear optical imaging of live cells by second harmonic generation. *Biophys J*. 1999;77:3341-9.
25. Burgeson RE. Basement Membranes. In: Fitzpatrick TB, Eisen AZ, Wolff K, Freedberg IM, Austen KF, editors. *Dermatology in General Medicine*. New York, NY: McGraw-Hill; 1987. p. 288-303.
26. Grinnell F, Toda K-I, Lamke-Seymour C. Reconstitution of human epidermis in vitro is accompanied by transient activation of basal keratinocyte spreading. *Exp Cell Res*. 1987;172:439-49.
27. Carter WG, Symington BE, Kaur P. Cell adhesion and the basement membrane in early epidermal morphogenesis. In: Fleming TP, editor. *Epithelial Organization and Development*. London: Chapman and Hall; 1992. p. 299-327.
28. Ekblom P. Basement membranes in development. In: Rohrbach DH, Timpl R, editors. *Molecular and Cellular Aspects of Basement Membranes*. New York, New York: Academic Press; 1993. p. 359-83.
29. Uitto J, Mauviel A, McGrath J. The Dermal-Epidermal Basement Membrane Zone in Cutaneous Wound Healing. In: Clark RAF, editor. *The Molecular and Cellular Biology of Wound Healing*. New York, NY: Plenum Press; 1996. p. 513-60.

30. Badgwell DB, Lu Z, Le K, Gao F, Yang M, Suh GK, Bao JJ, Das P, Andreeff M, Chen W, Yu Y, Ahmed AA, W SLL, Bast RC, Jr. The tumor-suppressor gene ARHI (DIRAS3) suppresses ovarian cancer cell migration through inhibition of the Stat3 and FAK/Rho signaling pathways. *Oncogene*. 2012;31(1):68-79. Epub 2011/06/07. doi: 10.1038/onc.2011.213 PubMed PMID: 21643014; PubMed Central PMCID: PMC3170676.
31. Liotta LA, Stetler-Stevenson WG. Tumor invasion and metastasis: an imbalance of positive and negative regulation. *Cancer Res*. 1991;51(18 Suppl):5054s-9s. Epub 1991/09/15. PubMed PMID: 1884381.
32. Ajeti V, Lien CH, Chen SJ, Su PJ, Squirrell JM, Molinarolo KH, Lyons GE, Eliceiri KW, Ogle BM, Campagnola PJ. Image-inspired 3D multiphoton excited fabrication of extracellular matrix structures by modulated raster scanning. *OPT EXPRESS*. 2013;21(21):25346-55. doi: Doi 10.1364/Oe.21.025346. PubMed PMID: ISI:000326085600090.
33. Kapur A, Felder M, Fass L, Kaur J, Czarnecki A, Rathi K, Zeng S, Osowski KK, Howell C, Xiong MP, Whelan RJ, Patankar MS. Modulation of oxidative stress and subsequent induction of apoptosis and endoplasmic reticulum stress allows citral to decrease cancer cell proliferation. *Scientific reports*. 2016;6:27530. doi: 10.1038/srep27530. PubMed PMID: 27270209; PubMed Central PMCID: PMC4897611.
34. Li HH, Zhao YJ, Li Y, Dai CF, Jobe SO, Yang XS, Li XF, Patankar MS, Magness RR, Zheng J. Estradiol 17beta and its metabolites stimulate cell proliferation and antagonize ascorbic acid-suppressed cell proliferation in human ovarian cancer cells. *Reprod Sci*. 2014;21(1):102-11. doi: 10.1177/1933719113492211. PubMed PMID: 23757313; PubMed Central PMCID: PMC43857769.
35. Wang K, Li Y, Jiang YZ, Dai CF, Patankar MS, Song JS, Zheng J. An endogenous aryl hydrocarbon receptor ligand inhibits proliferation and migration of human ovarian cancer cells. *Cancer Lett*. 2013;340(1):63-71. doi: 10.1016/j.canlet.2013.06.026. PubMed PMID: 23851185; PubMed Central PMCID: PMC43781955.
36. Liu Y, Whelan RJ, Pattnaik BR, Ludwig K, Subudhi E, Rowland H, Claussen N, Zucker N, Uppal S, Kushner DM, Felder M, Patankar MS, Kapur A. Terpenoids from *Zingiber officinale* (Ginger) induce apoptosis in endometrial cancer cells through the activation of p53. *PLoS One*. 2012;7(12):e53178. doi: 10.1371/journal.pone.0053178. PubMed PMID: 23300887; PubMed Central PMCID: PMC43534047.
37. Xiang X, Feng M, Felder M, Connor JP, Man YG, Patankar MS, Ho M. HN125: A Novel Immunoadhesin Targeting MUC16 with Potential for Cancer Therapy. *J Cancer*. 2011;2:280-91. PubMed PMID: 21611109; PubMed Central PMCID: PMC43100680.
38. Gubbels JA, Felder M, Horibata S, Belisle JA, Kapur A, Holden H, Petrie S, Migneault M, Rancourt C, Connor JP, Patankar MS. MUC16 provides immune protection by inhibiting synapse formation between NK and ovarian tumor cells. *Mol Cancer*. 2010;9:11. doi: 10.1186/1476-4598-9-11. PubMed PMID: 20089172; PubMed Central PMCID: PMC42818693.
39. Goodell CA, Belisle JA, Gubbels JA, Migneault M, Rancourt C, Connor J, Kunnimalaiyaan M, Kravitz R, Tucker W, Zwick M, Patankar MS. Characterization of the tumor marker muc16 (ca125) expressed by murine ovarian tumor cell lines and identification of a panel of cross-reactive monoclonal antibodies. *J Ovarian Res*. 2009;2(1):8. doi: 10.1186/1757-2215-2-8. PubMed PMID: 19538730; PubMed Central PMCID: PMC42708168.
40. Dell A, Chalabi S, Easton RL, Haslam SM, Sutton-Smith M, Patankar MS, Lattanzio F, Panico M, Morris HR, Clark GF. Murine and human zona pellucida 3 derived from mouse eggs express identical O-glycans. *Proc Natl Acad Sci U S A*. 2003;100(26):15631-6. doi: 10.1073/pnas.2635507100. PubMed PMID: 14673092; PubMed Central PMCID: PMC4307619.
41. Kim D, So PT. High-throughput three-dimensional lithographic microfabrication. *Opt Lett*. 2010;35(10):1602-4. Epub 2010/05/19. doi: 199321 [pii]. PubMed PMID: 20479822.

42. Lubeck E, Coskun AF, Zhiyentayev T, Ahmad M, Cai L. Single-cell in situ RNA profiling by sequential hybridization. *Nat Methods*. 2014;11(4):360-1. doi: 10.1038/nmeth.2892. PubMed PMID: 24681720; PubMed Central PMCID: PMC4085791.